Inorganic Chemistry

ARTICLE

pubs.acs.org/IC

Coordination Properties of 2,5-Dimesitylpyridine: An Encumbering and Versatile Ligand for Transition-Metal Chemistry

Julia M. Stauber, Andrew L. Wadler, Curtis E. Moore, Arnold L. Rheingold, and Joshua S. Figueroa*

Department of Chemistry and Biochemistry, University of California, San Diego, 9500 Gilman Drive, Mail Code 0358, La Jolla, California 92093-0358, United States

Supporting Information

ABSTRACT: To overcome the unfavorable steric pressures associated with 2,6-disubstitution in encumbering pyridine ligands, the coordination chemistry of a 2,5-disubstituted variant, namely, 2,5-dimesitylpyridine (2,5-Mes_2py), is reported. This diaryl pyridine shows good binding ability to a range of transition-metal fragments with varying formal oxidation states and coligands. Treatment of 2.0 equiv of 2,5-Mes_2py with monovalent Cu and Ag triflate sources generates complexes of the type [M(2,5-Mes_2py)$_2$]OTf (M = Cu, Ag; OTf = OSO_2CF_3), which feature long M-OTf distances and a substrate-accessible primary coordination sphere. Combination of 2,5-Mes_2py with Cu(OTf)$_2$ and Pd(OAc)$_2$ produces four-coordinate complexes featuring *cis*- and *trans*-2,5-Mes_2py orientations, respectively. The four-coordinate palladium complex Pd(OAc)$_2$(2,5-Mes_2py)$_2$ is found to resist py-ligand dissociation at room temperature in solution, but functions as a precatalyst for the aerobic C−H bond olefination of benzene at elevated temperatures. This C−H bond activation chemistry is compared with a similar Pd-based system featuring 2,6-disubstituted pyridines. 2,5-Mes_2py also readily supports mono- and dinuclear divalent Co complexes, and the solution-phase equilibria between such species are detailed. The coordination studies presented highlight the potential of 2,5-Mes_2py to function as an encumbering ancillary for the stabilization of low-coordinate complexes and as a supporting ligand for metal-mediated transformations.

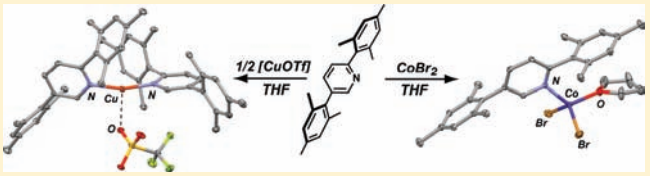

INTRODUCTION

As a result of its good binding ability and the moderately strong ligand field it provides, pyridine (py) is a ubiquitous ligand in transition-metal chemistry. While many substituted, monodentate pyridines have found wide utility as ligands, sterically encumbering 2,6-diaryl pyridines have received little attention. Indeed, for this class of pyridine ligands, only two variants have been reported, namely, the 2,6-dimesityl and 2,6-triisopropylphenyl derivatives, 2,6-Mes_2py and 2,6-$Tripp_2$py, respectively (Mes = 2,4,6-$Me_3C_6H_2$; Tripp = 2,4,6-(*i*-Pr)$_3C_6H_2$).[1,2] However, the transition-metal coordination chemistry of these ligands is limited to the monovalent-silver complex, [Ag(2,6-Mes_2py)$_2$]OTf (OTf = trifluoromethanesulfonate).[1] This lack of attention is not surprising given that 2,6-lutidine (2,6-Me_2py), although able to form isolable complexes,[3−8] binds transition metals with markedly low affinity because of the steric pressures posed by its 2,6-methyl groups.[9,10]

Although underexplored, the 2,6-diaryl pyridine framework is attractive because of its topological relationship to substituted *m*-terphenyl σ-aryl ligands ([2,6-$Ar_2C_6H_3$]$^-$; Ar = aryl, Chart 1),[11−14] which have been successfully employed as encumbering ancillaries for low-coordinate transition-metal complexes.[15−17] Indeed, use of the common, 2,6-dimesityl-substituted *m*-terphenyl ligand (i.e., 2,6-$Mes_2C_6H_3$)[18] has allowed for the isolation and structural characterization of two-coordinate, divalent Mn, Fe, and Co complexes of the simple formulation M(Ar)$_2$.[19,20] Further, use of the more encumbering 2,6-$Dipp_2C_6H_3$ *m*-terphenyl ligand (Dipp = 2,6-(*i*-Pr)$_2C_6H_3$)[21,22] enabled Power's discovery of the Cr−Cr dimer, Cr_2(2,6-$Dipp_2$-C_6H_3)$_2$, which was the first example of a complex possessing 5-fold bonding between two metal centers.[14,23−27]

Encumbering diaryl pyridines may similarly be expected to foster low-coordination numbers, but in a manner that does not require a metal valence unit for bonding. This feature is important for preserving additional redox equivalents for multielectron, metal-based transformations or catalysis. Thus, in an effort to avoid the potential binding limitations of 2,6-aryl pyridines, we reasoned that 2,5-diaryl substitution of a pyridine ring might maintain the encumbering environment offered by the terphenyl framework, while minimizing the steric pressures that lead to poor pyridine binding (Chart 1). Accordingly, herein we report the efficacy of this substitution strategy by introducing the 2,5-dimesityl pyridine derivative, 2,5-Mes_2py (Mes = 2,4,6-$Me_3C_6H_2$), and show that it can support a range of structurally diverse transition-metal complexes and C−H bond functionalization catalysis.

RESULTS AND DISCUSSION

Scheme 1 shows a straightforward route to 2,5-dimesitylpyridine based on Kumada-type cross-coupling. This procedure is similar to that reported for 2,6-dimesitylpyridine and provides the desired 2,5-Mes_2py ligand in 71% yield when employing

Received: April 28, 2011
Published: June 28, 2011

Chart 1. Topological Correlation between *m*-Terphenyl, 2,6-Diaryl Pyridine, and 2,5-Diaryl Pyridine Ligands[a]

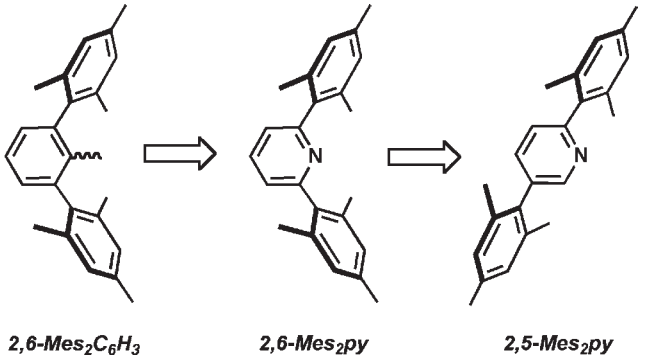

[a]The dimesityl derivative of each is used as an example.

Scheme 1

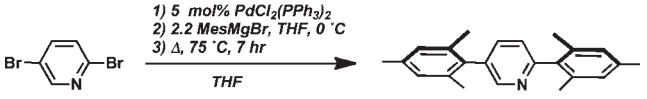

about 5.0 g of 2,5-dibromopyridine. Upon isolation, Mes_2py is obtained as a colorless, air-stable crystalline solid that is freely soluble in common organic solvents. Crystallographic characterization of 2,5-Mes_2py was complicated by end-over-end positional disorder of the nitrogen atom and *para* C−H unit and thus inhibited an accurate determination of the metrical parameters for the py ring (Supporting Information, Figure S3). However, the symmetrically distinct mesityl groups in 2,5-Mes_2py are readily apparent in its ^{1}H NMR spectrum (C_6D_6), which displays nine unique resonances. The solution IR spectrum of 2,5-Mes_2py (C_6D_6) exhibits moderately strong bands at 1610, 1587, and 1467 cm^{-1} which are in the range and intensity expected for C═N and C═C stretching modes.[28]

In analogy to its 2,6-substituted counterpart, 2,5-Mes_2py readily forms a bis-pyridine complex with monovalent Ag centers. As shown in Scheme 2, treatment of 2,5-Mes_2py with AgOTf in tetrahydrofuran (THF) solution provides the salt [Ag(2,5-$Mes_2py)_2$]OTf (1) as determined by X-ray diffraction (Figure 1). Interestingly, the solid-state structure of 1 possesses markedly long bond distances between the Ag center and the OTf^- oxygen atoms (Ag1−O1 = 2.876(2) Å, Ag1−O2 = 2.779(2) Å). While we contend that these Ag−O contacts are non-negligible, they are near the limit of a bonding interaction between the metal center and the OTf anion and likely reflect the strong σ-donating properties of the 2,5-Mes_2py ligand.[29] However, whereas the metal primary coordination sphere is inaccessible to the OTf^- ion in [Ag(2,6-$Mes_2py)_2$]OTf,[1] two 2,5-Mes_2py ligands clearly allow close approach of the counterion to the Ag center. This feature is significant in that both [Ag(2,6-$Mes_2py)_2$]OTf and **1** maintain near-linear N−Ag−N angles (178.1(2)° vs 164.29(7)°, respectively), but differ in their ability to accommodate additional ligands. We believe this highlights the prospects for substrate activation chemistry in the protected, yet accessible, 2,5-Mes_2py system.

Most importantly, 2,5-Mes_2py can bind to a range of other transition metals and is compatible with several other ligands. For example, treatment of 2,5-Mes_2py with (μ-C_6H_6)[Cu(OTf)]$_2$ in

Scheme 2

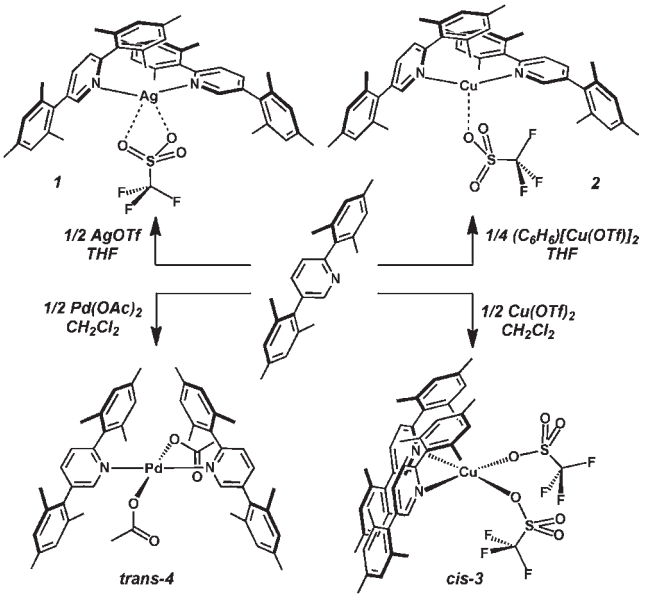

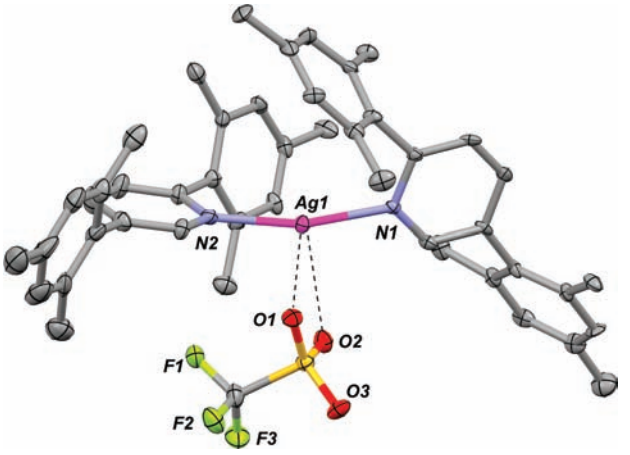

Figure 1. Molecular Structure of [Ag(2,5-$Mes_2py)_2$]OTf (**1**). Selected distances (Å) and angles (deg): Ag1−N1 = 2.1556(19), Ag1−N2 = 2.1523(19), Ag1−O1 = 2.876(2), Ag1−O2 = 2.779(2), N1−Ag1−N2 = 164.29(7).

THF solution generates the colorless complex [Cu(2,5-$Mes_2py)_2$]-OTf (**2**) as determined by X-ray diffraction (Scheme 2, Figure 2). The overall structural features of **2** are analogous to its Ag congener **1**, and it similarly possesses a long interaction between the monovalent metal center of the OTf^- counterion (d(Cu1−O1) = 2.423(3) Å). As expected, Cu-OTf distances contract substantially when the valence of the metal center is increased. Thus treatment of 2 equiv of 2,5-Mes_2py with the divalent copper source Cu(OTf)$_2$ in CH_2Cl_2 solution exclusively provides the *cis*-isomer of Cu(OTf)$_2$(2,5-$Mes_2py)_2$ (*cis*-**3**) as a green paramagnetic crystalline solid (μ_{eff} = 1.8(1) μ_B, Evans Method, $CDCl_3$/$(Me_3Si)_2O$, 20 °C, Scheme 2). Structural characterization of *cis*-**3** revealed Cu1−O1 and Cu1−O2 distances of 1.989(3) Å and 1.945(3) Å, respectively, which are indicative of Cu−O single bonds (Figure 3). Notably, a slight elongation of the Cu−N distances is observed in *cis*-**3** relative to **2** (1.990 Å (av) vs 1.907 Å

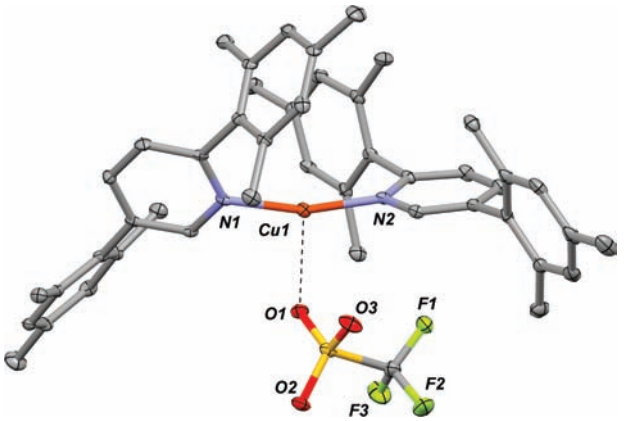

Figure 2. Molecular Structure of $[Cu(2,5\text{-}Mes_2py)_2]OTf$ (**2**). Selected distances (Å) and angles (deg): Cu1−N1 = 1.900(3), Cu1−N2 = 1.906(3), Cu1−O2 = 2.423(3), N1−Cu1−N2 = 164.05(11), N1−Cu1−O2 = 100.71(10), N2−Cu1−O2 = 94.99(10).

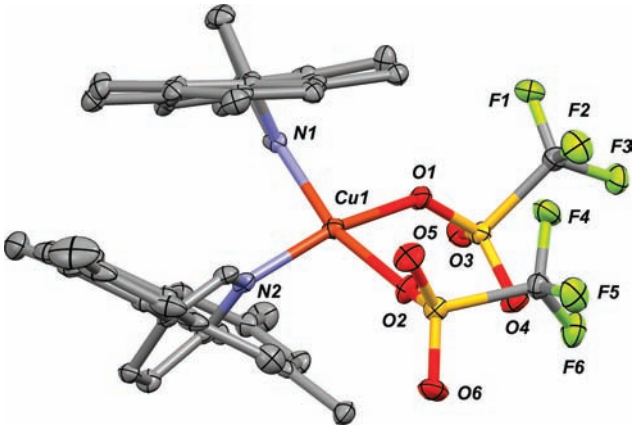

Figure 3. Molecular Structure of $Cu(OTf)_2(2,5\text{-}Mes_2py)_2$ (*cis*-**3**). Selected distances (Å) and angles (deg): Cu1−O1 = 1.989(3), Cu1−O2 = 1.945(3), Cu1−N1 = 1.995(4), Cu1−N2 = 1.985(4), O1−Cu1−O2 = 87.54(15), N1−Cu1−N2 = 99.47(16), O1−Cu1−N1 = 164.48(16), N1−Cu1−O2 = 84.39(15), O2−Cu1−N1 = 91.99(16), O2−Cu1−N2 = 163.93(16).

(av)). While this lengthening may reflect electronic destabilization between the nitrogen atoms and the Cu(II) singly occupied $d_{x^2-y^2}$ orbital, steric pressures between the *cis*-disposed 2,5-Mes_2py ligands likely also contribute to the observed Cu−N bond distances in *cis*-**3**. Supporting this notion is the fact that the related Cu(II) bis-triflate, bis-oxazoline complex $Cu(OTf)_2(\kappa^2\text{-}N,N\text{-}(S,S\text{-}i\text{-}Pr_2box^{Bz2}))$[30] ($S,S$-*i*-$Pr_2box^{Bz2}$ = [(4*S*,4′*S*)-4,4′,5,5′-tetrahydro-4,4′-diisopropyl-2,2′-(dibenzylmethylene)dioxazole]) exhibits Cu−N bond distances (d(Cu−N) = 1.941 Å (av)) that are slightly shorter than those in *cis*-**3**. We believe these shorter distances arise because the planar, *cis*-chelating S,S-*i*-Pr_2box^{Bz2} ligand poses less steric encumbrance around the Cu center relative to two *cis*-disposed 2,5-Mes_2py units. Interestingly, *cis*-**3** and $Cu(OTf)_2(\kappa^2\text{-}N,N\text{-}(S,S\text{-}i\text{-}Pr_2box^{Bz2}))$ represent the only four-coordinate Cu(II) bis-triflate complexes supported by nitrogen-based ligands to be structurally characterized, whereas many five- and six-coordinate complexes have been reported.[31]

In contrast to *cis*-**3**, a *trans*-disposed complex is dominant upon coordination of two 2,5-Mes_2py ligands to palladium(II)

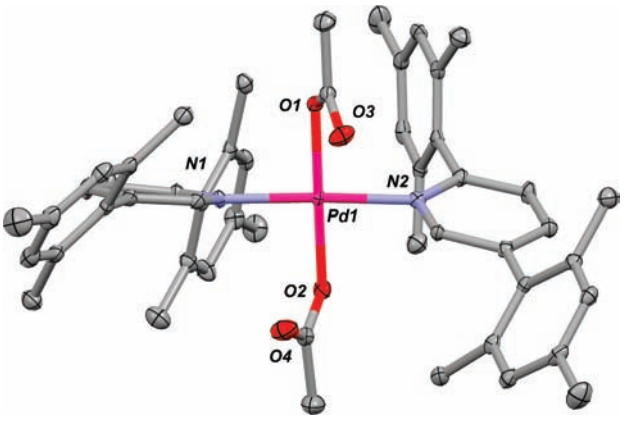

Figure 4. Molecular Structure of $Pd(OAc)_2(2,5\text{-}Mes_2py)_2$ (*trans*-**4**). Selected distances (Å) and angles (deg): Pd1−O1 = 2.0151(17), Pd1−O2 = 2.0078(18), Pd1−N1 = 2.029(3), Pd1−N2 = 2.031(3), O1−Pd1−O2 = 176.00(7), N1−Pd1−N2 = 171.91(11), O1−Pd1−N1 = 87.84(12), O1−Pd1−N2 = 91.94(12), O2−Pd(1)-N1 = 93.17(11), O2−Pd1−N2 = 87.60(11).

acetate. Addition of 2 equiv of 2,5-Mes_2py to $Pd(OAc)_2$ in CH_2Cl_2 solution provides a mixture of two species in a 20:1 ratio. Selective crystallization from Et_2O solution, followed by single-crystal X-ray diffraction revealed the major product to be *trans*-$Pd(OAc)_2(2,5\text{-}Mes_2py)_2$ (*trans*-**4**, Scheme 2, Figure 4). Although not isolated from the reaction mixture, we presume that the minor product is the *cis*-isomer of $Pd(OAc)_2(2,5\text{-}Mes_2py)_2$, because it exhibits a 1:1 ratio of acetate to 2,5-Mes_2py ^{1}H NMR resonances.[32] When monitored over the course of 5 days, these complexes do not interconvert in solution (C_6D_6) in a manner that alters the initial product distribution.

Monomeric *trans*-**4** is most structurally comparable to the complex $Pd(OAc)_2(2,6\text{-}i\text{-}Oct_2py)_2$ (*i*-Oct = isooctyl) reported by Yu in the context of Pd-catalyzed aerobic aryl−C-H bond olefination.[33] Interestingly, 2,6-dialkyl substituted $Pd(OAc)_2(2,6\text{-}i\text{-}Oct_2py)_2$ was proposed to undergo a ligand-dissociation/dimerization sequence in $CDCl_3$ solution at room temperature to the bridging-acetate dimer $[\mu\text{-}(\kappa^2\text{-}OAc)Pd(OAc)(2,6\text{-}i\text{-}Oct_2py)]_2$. The latter results from dimerization of the three-coordinate, monopyridine intermediate $[Pd(OAc)_2(2,6\text{-}i\text{-}Oct_2py)]$, which is presumably responsible for the electrophilic C−H activation of aryl substrates during catalysis.[34−36] In contrast, *trans*-**4** is stable for extended periods at room temperature in both $CDCl_3$ and C_6D_6 solution, which further highlights the difference in steric pressure between 2,6- and 2,5-substitution of the pyridine framework. Interestingly, heating of *trans*-**4** in C_6D_6 solution to 60 °C for 2 h results in about 15% decomposition to free 2,5-Mes_2py (^{1}H NMR), with insoluble black precipitates noticeable in the reaction mixture. However, thermolysis does not result in the formation of an observable new species as assayed by ^{1}H NMR spectroscopy, and full decomposition is achieved under these conditions after approximately 24 h.

Despite the fact that ligand dissociation is not readily observed from *trans*-**4**, it can indeed catalyze aerobic C−H bond olefination. Accordingly, benzene and ethyl acrylate are readily coupled to *trans*-ethyl cinnamate in 74% isolated yield using 10 mol % of *trans*-**4** in the presence of acetic anhydride (Ac_2O) and O_2 (Scheme 3).[37,38] When using benzene as both the substrate and the solvent, this transformation occurs at 60 °C over the course of 6 h, which represents fairly mild conditions for an

Scheme 3

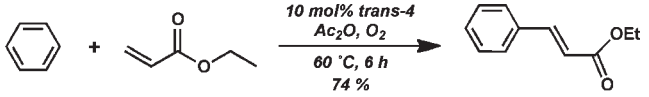

Scheme 4

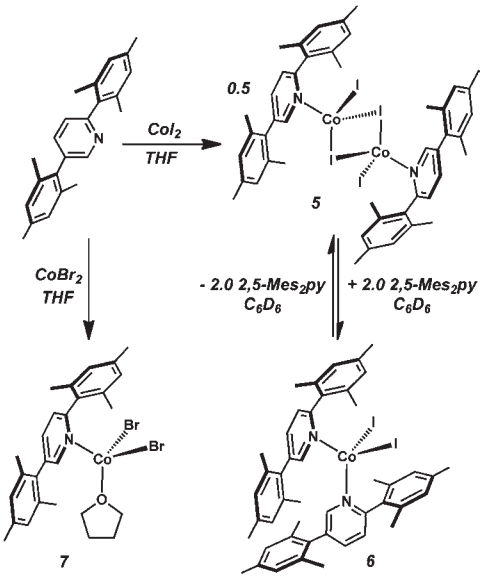

aerobic C−H bond olefination reaction.[32,39−43] Thus, we believe that the thermolysis study of *trans*-**4** in C_6D_6 above results in the formation of products stemming from C-D activation, which decompose in the absence of arene-coupling partners and additives. Notably, 1:2 in situ mixing of $Pd(OAc)_2$ and 2,5-Mes_2py (10 mol % [Pd]), the approach typical for such olefination reactions, results in slightly lower yield for the coupling of benzene and ethyl acrylate relative to preformed *trans*-**4** under similar conditions (67%).

The encumbering 2,5-Mes_2py ligand also displays intriguing coordination properties and solution behavior in conjunction with divalent cobalt halides. For example, treatment of CoI_2 with 1 equiv of 2,5-Mes_2py in THF solution results in the green, bridging-diiodide dimer, $[(\mu\text{-I})CoI(2,5\text{-}Mes_2py)]_2$ (**5**) as determined by X-ray diffraction (Scheme 4, Figure 5). Interestingly, Evans Method magnetic moment determination on **5** ($C_6D_6/(Me_3Si)_2O$, 20 °C) resulted in a μ_{eff} value of 5.9(2) μ_B, which indicates an overall S = 2 ground state for the dimer. Nominally tetrahedral divalent Co centers are well-known to exhibit quartet, S = 3/2 ground states when ligated to weak to moderate field ligands.[44] Thus, the magnetic data for **5** suggest that it features antiferromagnetic coupling of two unpaired spins across the bridging-diiodide core and, correspondingly, that its dimeric formulation remains intact in solution.

Notably, **5** is reminiscent of the bridging diacetate dimer $[\mu\text{-}(\kappa^2\text{-}OAc)Pd(OAc)(2,6\text{-}i\text{-}Oct_2py)]_2$ spectroscopically observed by Yu upon ligand dissociation from *trans*-$Pd(OAc)_2$-$(2,6\text{-}i\text{-}Oct_2py)_2$. While similar behavior is not observed for the palladium complex *trans*-**4**, dimer **5** does engage in ligand association/dimerization equilibria in the presence of added 2,5-Mes_2py. Accordingly, addition of 2 equiv of 2,5-Mes_2py to

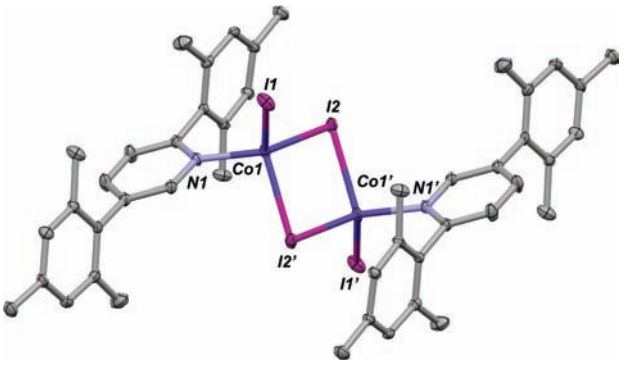

Figure 5. Molecular Structure of $[(\mu\text{-I})CoI(2,5\text{-}Mes_2py)]_2$ (**5**, note crystallographic inversion symmetry). Selected distances (Å) and angles (deg): Co1−I1 = 2.5497(9), Co1−I2 = 2.6284(9), Co1−N1 = 2.033(4), Co1−I2′ = 2.6533(9), I2−Co1′ = 2.6533(9), Co1−I2−Co1′ = 83.79(3), N1−Co1−I1 = 105.38(13), N1−Co1−I2 = 125.70(12), I1−Co1−I2 = 110.63(3), N1−Co1−I2′ = 100.40(11), I1−Co1−I2′ = 118.96(3), I2−Co1−I2′ = 96.21(3).

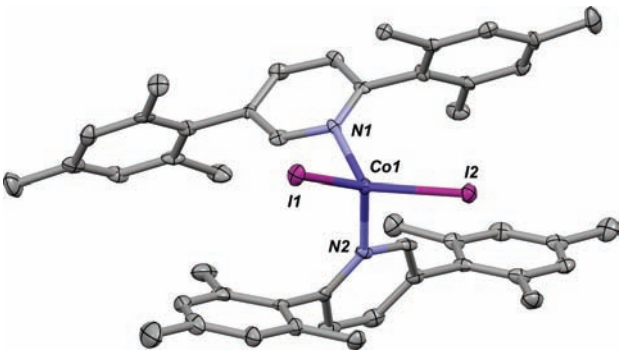

Figure 6. Molecular Structure of $CoI_2(2,5\text{-}Mes_2py)_2$ (**6**, only one crystallographically, but chemically equivalent, molecule shown). Selected distances (Å) and angles (deg): Co1−I1 = 2.5658(10), Co1−I2 = 2.5495(10), Co1−N1 = 2.074(5), Co1−N2 = 2.082(5), N1−Co1−N2 = 92.3(2), N1−Co1−I2 = 103.11(14), N1−Co1−I1 = 125.56(15), N2−Co1−I1 = 100.27(15), N2−Co1−I2 = 126.44(16), I2−Co1−I1 = 110.38(4).

bridging diiodide **5** in C_6D_6 creates an equilibrium mixture between the starting materials and the paramagnetic monomer, $CoI_2(2,5\text{-}Mes_2py)_2$ (**6**), with K_{eq} = 1.0(1) at 25 °C.[45] Addition of 4 equiv of 2,5-Mes_2py to dimer **5** shifts the equilibrium constant to K_{eq} = 1.7(4), which is sufficient to isolate **6** by crystallization from an Et_2O/THF mixture at −35 °C. Crystallographic characterization of **6** confirmed its identity (Figure 6) and revealed a four-coordinate cobalt center that deviates significantly from ideal tetrahedral symmetry according to Houser's τ_4 four-coordinate geometry index (τ_4 geometry index = 0.79 (av)).[44,46]

The speciation of cobalt-2,5-Mes_2py complexes can also be modulated by the Lewis acidity properties of the Co center. Whereas equimolar mixtures of 2,5-Mes_2py and CoI_2 form dimer **5** in THF solution, a similar protocol employing $CoBr_2$ produces the monomer $CoBr_2(THF)(2,5\text{-}Mes_2py)$ (**7**) as the exclusive product (Scheme 4). We believe that the greater Lewis acidity[47,48] of the cobalt center in CoI_2 is not effectively quenched by THF relative to $CoBr_2$, and thus results in dimer formation. However, when **7** is dissolved in C_6D_6, free THF is apparent in the ^{1}H NMR spectrum and a μ_{eff} value of 6.3(2) μ_B is

dx.doi.org/10.1021/ic201205p |*Inorg. Chem.* 2011, 50, 7309–7316

Scheme 5

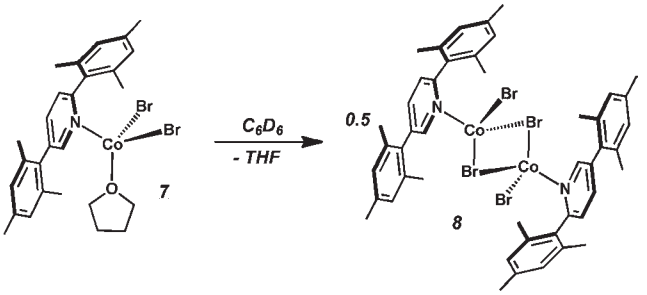

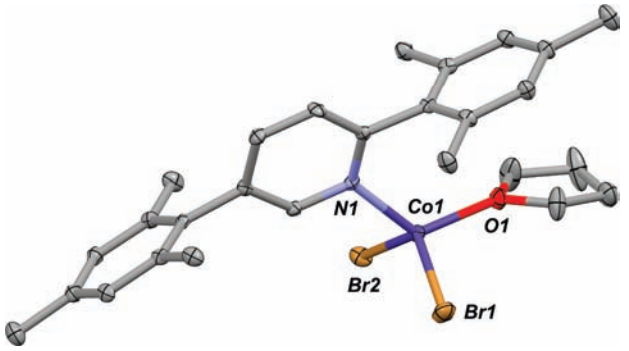

Figure 7. Molecular Structure of $CoBr_2(THF)(2,5\text{-}Mes_2py)$ (**7**). Selected distances (Å) and angles (deg): Co1−O1 = 1.989(3), Co1−N1 = 2.040(3), Co1−Br1 = 2.3959(9), Co1−Br2 = 2.3638(9), O1S−Co1−N1 = 124.41(14), O1−Co1−Br2= 105.10(10), O1−Co1−Br1= 103.92(10), N1−Co1−Br1= 101.60(10), N1−Co1−Br2 = 101.30(10), Br1−Co1−Br1 = 122.31(3).

obtained. We believe these observations are indicative of the formation of the $S = 2$ dimer, $[(\mu\text{-Br})CoBr(2,5\text{-}Mes_2py)]_2$ (**8**), in absence of excess THF (Scheme 5). Indeed, the ^1H NMR spectrum of monomer **7** in C_6D_6 solution is nearly identical to that of the diiodide dimer **5**, which further suggests that dimerization to **8** occurs when THF is not present in excess.[49] Nevertheless, the monomeric nature of **7** as obtained from THF solution is intriguing (Figure 7), as only one other example of a neutral monomer with the relatively simple formulation $CoX_2(THF)L$ has been structurally characterized (X = halide).[50,51]

CONCLUDING REMARKS

In conclusion, 2,5-dimesityl substitution results in a diaryl pyridine that is capable of ligating a range of transition-metal fragments. The structural properties of the complexes reported here demonstrate that the $2,5\text{-}Mes_2py$ ligand provides an encumbering steric environment, but also readily allows substrate access to central metal atoms. In this respect, 2,5-diaryl substitution of a pyridine ring is an effective strategy for minimizing the steric pressures that are known to attenuate effective binding of 2,6-disubstitued pyridines in general. Such enhanced binding is critical for a pyridine ligand aiming to emulate the topological properties of the *m*-terphenyl framework, especially given a neutral, rather than anionic, bonding mode. However, topologically similar, yet neutral variants of the *m*-terphenyl framework are appealing to further increase the multielectron redox activity of a low-coordinate metal center. We believe $2,5\text{-}Mes_2py$ and other 2,5-diaryl pyridines may be particularly useful in this regard and are exploring further the reactivity of their transition-metal complexes.

EXPERIMENTAL SECTION

General Considerations. All manipulations were carried out under an atmosphere of dry dinitrogen using standard Schlenk and glovebox techniques. Solvents were dried and deoxygenated according to standard procedures. Unless otherwise stated, reagent grade starting materials were purchased from commercial sources and used as received or purified by standard procedures. Benzene-d_6 and chloroform-*d* (Cambridge Isotope Laboratories) were degassed and stored over 4 Å molecular sieves for 2 d prior to use. Celite 405 (Fisher Scientific) was dried under vacuum (24 h) at a temperature above 250 °C and stored in the glovebox prior to use.

Solution ^1H, $^{13}C\{^1H\}$, and $^{19}F\{^1H\}$ spectra were recorded on Varian Mercury 300 and 400 spectrometers, a Varian X-Sens500 spectrometer or a JEOL ECA-500 spectrometer. ^1H and $^{13}C\{^1H\}$ chemical shifts are reported in ppm relative to $SiMe_4$ (^1H and ^{13}C $\delta = 0.0$ ppm) with reference to residual solvent resonances of 7.16 ppm (^1H) and 128.06 ppm (^{13}C) for benzene-d_6 and 7.26 ppm (^1H) for chloroform-*d*.[52] $^{19}F\{^1H\}$NMR spectra were referenced externally to neat trifluoroacetic acid, $F_3CC(O)OH$ ($\delta = -78.5$ ppm vs $CFCl_3 = 0.0$ ppm). FTIR spectra were recorded on a Thermo-Nicolet iS10 FTIR spectrometer. Samples were prepared as C_6D_6 solutions injected into a ThermoFisher solution cell equipped with KBr windows. For solution FTIR spectra, solvent peaks were digitally subtracted from all spectra by comparison with an authentic spectrum obtained immediately prior to that of the sample. The following abbreviations were used for the intensities and characteristics of important IR absorption bands: vs = very strong, s = strong, m = medium, w = weak, vw = very weak; b = broad, vb = very broad, sh = shoulder. Combustion analyses were performed by Robertson Microlit Laboratories of Madison, NJ (U.S.A.).

Synthesis of 2,5-Dimesitylpyridine ($2,5\text{-}Mes_2py$). To a THF solution of 2,5-dibromopyridine (5.380 g, 0.0227 mol, 100 mL) and $PdCl_2(PPh_3)_2$ (0.798 g, 0.00114 mol, 5 mol %) was added a 1 M THF solution of MesMgBr (0.050 mol, 50 mL) dropwise at 0 °C. Upon complete addition, the reaction mixture was allowed to warm to room temperature and then heated under reflux for 7 h at 75 °C. The reaction mixture was quenched by the dropwise addition of H_2O (20 mL) under an N_2 flow, and then poured over H_2O (200 mL). The organic materials were extracted with EtOAc (3 × 150 mL), washed with brine (20 mL), and then dried over $MgSO_4$. All volatile materials were then removed in vacuo. Flash chromatography using a 93:7 hexanes/EtOAc mixture provided a colorless residue. Crystallization of this material from hexanes at −20 °C, followed by thorough drying in vacuo, provided pure 2,5-dimesitylpyridine ($2,5\text{-}Mes_2py$) as a colorless crystalline solid. Yield: 5.085 g, 0.016 mol, 71.0%. ^1H NMR (400.1 MHz, C_6D_6, 20 °C): $\delta = 8.64$ (dd, 1H, $^4J = 2$ Hz, $^5J = 1$ Hz, *o*-py), 7.11 (dd, 1H, $^3J = 8$ Hz, $^4J = 2$ Hz, *p*-py), 6.94 (dd, 1H, $^3J = 8$ Hz, $^5J = 1$ Hz, *m*-py), 6.89 (s, 2H, *m*-Mes), 6.83 (s, 2H, *m*-Mes), 2.22 (s, 3H, *p*-CH_3-Mes), 2.19 (s, 3H, *p*-CH_3-Mes), 2.18 (s, 6H, *o*-CH_3-Mes), 1.99 (s, 6H, *o*-CH_3-Mes) ppm. $^{13}C\{^1H\}$ NMR (100.6 MHz, C_6D_6, 20 °C): δ = 159.0, 150.6, 138.8, 137.3, 137.2, 136.8, 136.2, 136.0, 135.8, 134.6, 128.7 (two resonances overlapping) 124.4, 21.2 (*p*-CH_3-Mes), 21.2 (*p*-CH_3-Mes), 20.9 (*o*-CH_3-Mes), 20.5 (*o*-CH_3-Mes) ppm. FTIR (C_6D_6, KBr windows): 3012 (m), 2968 (m), 2945 (m), 2919 (m), 2855 (m), 1610 (m), 1587 (m), 1543 (m), 1488 (m), 1467 (s), 1374 (w), 1365 (w, sh), 1328 (w), 1046 (vw), 1018 (w), 1000 (w), 849 (m) cm^{-1}. FTIR (KBr pellet): 3009 (m), 2967 (m), 2915 (m), 2855 (m), 2733 (w), 1612 (m), 1590 (m), 1546 (w), 1467 (s), 1375 (w), 1287 (w), 1123 (w), 1050 (w), 1021 (m), 998 (w), 945 (vw), 844 (m), 736 (w), 645 (w), 615 (w), 570 (m) cm^{-1}. Anal. Calcd. for $C_{23}H_{25}N$: C, 87.56; H, 7.99; N, 4.44. Found: C, 87.29; H, 8.24; N, 4.44.

dx.doi.org/10.1021/ic201205p |*Inorg. Chem.* 2011, 50, 7309–7316

Synthesis of [Ag(2,5-Mes$_2$py)$_2$]OTf (1). To a THF solution of 2,5-Mes$_2$py (0.079 g, 0.25 mmol, 2.1 equiv, 3 mL) was added a THF solution of AgOTf (0.031 g, 0.12 mmol, 3 mL) at room temperature. The colorless solution was stirred for 12 h, then filtered through Celite, followed by removal of THF under reduced pressure. Dissolution of the resulting colorless solid in 2 mL of Et_2O followed by filtration and storage at −35 °C for 24 h resulted in colorless crystals, which were collected and dried in vacuo. Yield: 0.073 g, 0.082 mmol, 68%. ^{1}H NMR (400.1 MHz, C_6D_6, 20 °C): δ = 8.50 (dd, 2H, ^4J = 2 Hz, ^5J =1 Hz, *o*-py), 6.96 (dd, 2H, ^3J = 8 Hz, ^4J = 2 Hz, *p*-py), 6.80 (s, 4H, *m*-Mes), 6.69 (m, 4H, *m*-Mes), 6.68 (dd, 2H, ^3J = 8 Hz, ^5J = 1 Hz, *m*-py), 2.17 (s, 6H, *p*-CH_3-Mes), 2.03 (s, 6H, *p*-CH_3-Mes), 2.02 (s, 12H, *o*-CH_3-Mes), 1.98 (s, 12H, *o*-CH_3-Mes) ppm. ^{13}C{^{1}H} NMR (100.6 MHz, C_6D_6, 20 °C): δ = 158.4, 153.0, 139.7, 138.6, 138.3, 138.0, 136.6, 136.3, 136.3, 133.9, 128.8, 124.6, 21.2 (*p*-CH_3-Mes), 21.0 (*p*-CH_3-Mes), 20.8 (*o*-CH_3-Mes), 20.1 (*o*-CH_3-Mes) ppm. ^{19}F{^{1}H} NMR (282.4 MHz, C_6D_6, 20 °C): δ = −77.6 ppm. FTIR (C_6D_6, KBr windows): 2959 (w, sh), 2924 (m), 2855 (w), 1613 (w), 1552 (vw), 1467 (w, sh), 1455 (w), 1386 (vw), 1377 (vw), 1328 (m), 1291 (m), 1242 (m), 1159 (m), 1053 (w), 1025 (m), 852 (w), 812 (vs), 664 (w), 634 (m) cm^{-1}. Anal. Calcd. for $C_{47}H_{50}N_2F_3O_3SAg$: C, 63.57; H, 5.68; N, 3.16. Found: C, 63.79; H, 5.70; N, 3.08.

Synthesis of [Cu(2,5-Mes$_2$py)$_2$]OTf (2). To a THF solution of (μ-C_6H_6)[CuOTf]$_2$ (0.036 g, 0.072 mmol, 3 mL) was added a THF solution of 2,5-Mes$_2$py (0.090 g, 0.29 mmol, 4.0 equiv, 3 mL) at room temperature. The reaction mixture was stirred for 36 h, filtered through Celite and all volatile materials were removed under reduced pressure. Dissolution of the resulting colorless residue in a 2:1 toluene/*n*-pentane mixture (2 mL) followed by filtration and storage at −35 °C for 24 h resulted in colorless crystals, which were collected and dried in vacuo. Yield: 0.042 g, 0.050 mmol, 69%. ^{1}H NMR (399.9 MHz, C_6D_6, 20 °C): δ = 8.19 (bd, 2H, ^4J = 2 Hz, *o*-py), 6.95 (dd, 2H, ^3J = 8 Hz, ^4J = 2 Hz, *p*-py), 6.82 (s, 4H, *m*-Mes), 6.68 (d, 2H, ^3J = 8 Hz, *m*-py), 6.66 (s, 4H, *m*-Mes), 2.19 (s, 6H, *p*-CH_3-Mes), 2.04 (s, 12H, *o*-CH_3-Mes), 2.02 (s, 12H, *o*-CH_3-Mes), 2.00 (s, 6H, *p*-CH_3-Mes) ppm. ^{13}C{^{1}H} NMR (100.6 MHz, C_6D_6, 20 °C): δ = 157.8, 151.5, 139.2, 138.7, 138.1, 137.0, 136.7, 136.4, 136.3, 133.9, 128.8, 128.6, 125.1, 21.1 (*p*-CH_3-Mes), 20.9 (*p*-CH_3-Mes), 20.7 (*o*-CH_3-Mes), 20.3 (*o*-CH_3-Mes) ppm. ^{19}F{^{1}H} NMR (282.4 MHz, C_6D_6, 20 °C): δ = −78.3 ppm. FTIR (C_6D_6, KBr windows): 2971 (w), 2919 (w), 2863 (w), 1609 (w), 1551 (w, sh), 1468 (m), 1381 (w), 1294 (s), 1238 (s), 1216 (s, sh), 1160 (s), 1028 (s), 847 (m), 793 (w, sh), 639 (s), 574 (w) cm^{-1}. Anal. Calcd. for $C_{47}H_{50}N_2F_3O_3SCu$: C, 66.92; H, 5.98; N 3.32. Found: C, 66.71; H, 6.21; N 3.32.

Synthesis of Cu(OTf)$_2$(2,5-Mes$_2$py)$_2$ (*cis*-3). To a CH_2Cl_2 solution of Cu(OTf)$_2$ (0.037 g, 0.10 mmol, 3 mL) was added a CH_2Cl_2 solution of 2,5-Mes$_2$py (0.065 g, 0.21 mmol, 2.0 equiv, 3 mL), which resulted in a gradual color change from colorless to green over the course of 12 h. The reaction mixture was stirred for a total of 36 h, then filtered through Celite and evaporated to dryness under reduced pressure. Dissolution of the resulting residue in C_6H_6 (2 mL) followed by filtration and storage at room temperature for 24 h resulted in green crystals, which were collected and dried in vacuo. Yield: 0.059 g, 0.059 mmol, 57%. ^{1}H NMR (400.1 MHz, C_6D_6, 20 °C): δ = 8.17 (bs, 2H, *o*-py), 6.85 (bm, 4H, *p*-py + *m*-py), 3.79 (bs, 8H, *m*-2-Mes+ *m*-5-Mes), 2.23 (bs, 6H, *p*-CH_3-Mes), 2.05 (bs, 12H, *o*-CH_3-Mes), 1.80 (bs, 6H, *p*-CH_3-Mes), 1.62 (bs, 12H, *o*-CH_3-Mes) ppm. Evans Method ($CDCl_3$ w/ ($Me_3Si)_2O$; 20 °C): μ_{eff} = 1.8(1) μ_B (average of 4 independent measurements). FTIR (C_6D_6, KBr windows): 3047 (w, sh), 2976 (w, br), 2924 (w), 2855 (w), 2387 (w, br), 1612 (w), 1554 (vw, sh), 1467 (w), 1381 (w, sh), 1299 (m), 1236 (w), 1219 (w, sh), 1163 (w), 1072 (vw), 1025 (m), 925 (w, br), 850 (w), 813 (m), 662 (vw, sh), 634 (m), 569 (vw) cm^{-1}. Anal. Calcd. for $C_{48}H_{50}F_6N_2O_6S_2Cu$: C, 58.07; H, 5.08; N, 2.82. Found: C, 57.80; H, 5.08; N, 2.57.

Synthesis of *trans*-Pd(OAc)$_2$(2,5-Mes$_2$py)$_2$ (*trans*-4). To a CH_2Cl_2 solution of Pd(OAc)$_2$ (0.028 g, 0.12 mmol, 3 mL) was added a CH_2Cl_2 solution of 2,5-Mes$_2$py (0.079 g, 0.25 mmol, 3 mL, 2.0 equiv). The yellow reaction mixture was allowed to stir for 16 h, and gradually darkened in color. The mixture was filtered through Celite and then all volatile materials were removed in vacuo. Dissolution of the resulting yellow residue in Et_2O (3 mL) followed by filtration and storage at −35 °C resulted in yellow crystals, which were collected and dried in vacuo. Yield: 0.065 g, 0.076 mmol, 61%. ^{1}H NMR (399.9 MHz, C_6D_6, 20 °C): δ = 10.28 (bd, 2H, ^4J = 2 Hz, *o*-py), 6.98 (s, 4H, *m*-Mes), 6.80 (dd, 2H, ^3J = 8 Hz, ^4J = 2 Hz, *p*-py), 6.70 (s, 4H, *m*-Mes), 6.49 (d, 2H, ^3J = 8 Hz, *m*-py), 2.47 (s, 6H, OC(O)CH_3), 2.13 (s, 6H, *p*-CH_3-Mes), 2.04 (s, 12H, *o*-CH_3-Mes), 2.02 (s, 12H, *o*-CH_3-Mes), 1.83 (s, 6H, *p*-CH_3-Mes) ppm. ^{13}C{ ^{1}H} NMR (100.6 MHz, C_6D_6 , 20 °C): δ = 176.2 (*C* =O), 160.3, 157.0, 138.9, 137.7, 137.5, 137.0, 136.2, 135.9, 135.5, 133.7, 128.8, 128.7, 125.8, 23.2 (OC(O)CH_3), 21.7 (*p*-CH_3-Mes), 21.1 (*p*-CH_3-Mes), 20.8 (*o*- CH_3-Mes), 20.4 (*o*-CH_3-Mes) ppm. FTIR (C_6D_6, KBr windows): $\nu_{(C=O)}$ 1642 (vs) cm^{-1}, also 2968 (w), 2918 (w), 2857 (w), 1616 (m), 1551 (w, sh), 1510 (vw), 1474 (m), 1374 (vw, sh), 1355 (m), 1316 (w, sh), 1305 (s), 1033 (w), 846 (m), 813 (m), 686 (w) cm^{-1}. Anal. Calcd. for $C_{50}H_{56}N_2O_4Pd$: C, 70.19; H, 6.60; N, 3.28. Found: C, 69.97; H, 6.59; N, 3.18.

Synthesis of [(μ-I)CoI(2,5-Mes$_2$py)]$_2$ (5). To a THF solution of 2,5-Mes$_2$py (0.058 g, 0.18 mmol, 3 mL, 1.0 equiv) was added a THF solution of CoI_2 (0.057 g, 0.18 mmol, 3 mL). The resulting green reaction mixture was stirred for 36 h, then filtered through Celite and evaporated to dryness under reduced pressure. The resulting green residue was washed with *n*-pentane (3 mL) and dried under reduced pressure. Dissolution of the resulting green solid in a toluene/*n*-pentane/THF mixture (2:2:1, 5 mL total) followed by filtration and storage at −35 °C for 24 h resulted in green crystals, which were collected and dried in vacuo. Yield: 0.085 g, 0.068 mmol, 74%. ^{1}H NMR (400.1 MHz, C_6D_6, 20 °C): δ = 7.71 (bs, 6H, *o*-py + *p*-py + *m*-py), 6.82 (bs, 8H, *m*-2-Mes + *m*-5-Mes), 2.37 (bs, 12H, *o*-CH_3-Mes), 1.44 (bs, 12H, *o*-CH_3-Mes), −4.92 (bs, 6H, *p*-CH_3-Mes), −5.86 (bs, 6H, *p*-CH_3-Mes) ppm. Evans Method (C_6D_6 w/ ($Me_3Si)_2O$; 20 °C): μ_{eff} = 5.9(2) μ_B (average of 6 independent measurements). FTIR (C_6D_6, KBr windows): 3087 (w, sh), 3060 (w, sh), 3027 (m), 2946 (w, sh), 2919 (m), 2859 (w, sh), 1605 (w), 1497 (s), 1466 (m), 1376 (w), 1077 (w), 1028 (w), 849 (w), 818 (w), 728 (vs), 692 (vs) cm^{-1}. Anal. Calcd. for $C_{46}H_{50}N_2Co_2I_4$: C, 43.95; H, 4.01; N, 2.23. Found: C, 44.70; H, 4.64; N, 1.89.

Synthesis of CoI$_2$(Mes$_2$py)$_2$ (6). To a THF solution of 2,5-Mes$_2$py (0.033 g, 0.10 mmol, 3 mL, 4.0 equiv) was added a THF solution of [(μ-I)CoI(2,5-Mes$_2$py)]$_2$ (**5**, 0.032 g, 0.026 mmol, 3 mL) at room temperature. The reaction mixture was stirred for 36 h, then filtered through Celite and evaporated to dryness under reduced pressure. Dissolution of the resulting green solid in a THF/Et_2O mixture (3:1, 4 mL total) followed by filtration and storage at −35 °C for 24 h resulted in a small amount of green crystals, which were collected and analyzed by single-crystal X-ray diffraction. Generation of CoI$_2$(Mes$_2$py)$_2$ for spectroscopic analysis was achieved via the addition of 4.0 equiv of 2,5-Mes$_2$py to [(μ-I)CoI(2,5-Mes$_2$py)]$_2$ (**5**) in C_6D_6 solution. The spectral data reported below were obtained in the presence of excess 2,5-Mes$_2$py. ^{1}H NMR (399.9 MHz, C_6D_6, 20 °C): δ = 13.65 (bs, 1H, *o*-py), 9.34 (bs, 1H, *m*-py), 8.50 (bs, 1H, *p*-py), 8.24 (bs, 2H, *m*-Mes) 3.49 (bs, 6H, *o*-CH_3-Mes), 0.58 (bs, 2H, *m*-Mes), 0.31 (bs, 6H, *o*-CH_3-Mes), −6.09 (bs, 12H, *p*-CH_3-Mes + *p*-CH_3-2-Mes) ppm. Satisfactory combustion analysis and Evans Method magnetic moment determination were not obtained for this complex because of the necessary presence of excess 2,5-Mes$_2$py.

Synthesis of CoBr$_2$(THF)(2,5-Mes$_2$py) (7). To a THF solution of 2,5-Mes$_2$py (0.037 g, 0.12 mmol, 3 mL, 1.0 equiv) was added a THF solution of $CoBr_2$ (0.026 g, 0.12 mmol, 3 mL). The reaction mixture was

stirred for 36 h, then filtered through Celite and evaporated to dryness under reduced pressure. The resulting blue residue was washed with *n*-pentane (3 mL) and dried under reduced pressure. Dissolution of the blue residue in a THF/*n*-pentane mixture (3:1, 2 mL total) and storage at −35 °C for 48 h resulted in blue crystals, which were collected and dried in vacuo. Analysis by ^{1}H NMR spectroscopy indicated the presence of free THF and resonances for the presumed dimer, $[(\mu\text{-Br})\text{CoBr}(2,5\text{-Mes}_2\text{py})]_2$ (**8**). Yield: 0.044 g, 0.073 mmol, 62%. ^{1}H NMR (400.1 MHz, C_6D_6, 20 °C): δ = 7.97 (bs, 3H, *o*-py+ *p*-py+ *m*-py), 6.89 (bs, 4H, *m*-Mes), 3.31 (bs, 4H, THF), 2.57 (bs, 6H, *o*-C*H*$_3$-Mes), 1.24 (bs, 6H, *o*-C*H*$_3$-Mes), 1.13 (bs, 4H, THF), −3.05 (bs, 3H, *p*-CH$_3$-Mes), −4.72 (bs, 3H, *p*-CH$_3$-Mes) ppm. Evans Method (C_6D_6 w/ $(Me_3Si)_2O$; 20 °C, on presumed $[(\mu\text{-Br})\text{CoBr}(2,5\text{-Mes}_2\text{py})]_2$): μ_{eff} = 6.3(2) μ_B (average of 4 independent measurements). FTIR (KBr pellet, on $\text{CoBr}_2(\text{THF})(2,5\text{-Mes}_2\text{py})$ solid): 2975 (w), 2950 (w), 2916 (w), 2859 (w, sh), 1610 (m), 1554 (w), 1508 (w), 1473 (m), 1378 (w), 1292 (w), 1228 (vw), 1167 (vw), 1132 (w), 1063 (w), 1018 (m), 919 (w), 865 (m), 855 (m), 735 (w), 666 (w), 619 (w), 572 (m) cm^{-1}. Anal. Calcd. for $C_{27}H_{33}NOCoBr_2$ ($\text{CoBr}_2(\text{THF})(2,5\text{-Mes}_2\text{py})$ solid): C, 53.47; H, 5.49; N, 2.31. Found: C, 53.37; H, 5.43; N, 2.25.

Benzene C−H Bond Olefination Reactions. *(a). Using trans-**4**.* In the glovebox, a 25 mL Teflon-capped reaction vessel was charged with *trans*-**4** (0.042 g, 0.049 mmol, 10 mol %) and a magnetic stir bar. The vessel was attached to an argon-charged Schlenk line, and acetic anhydride (45 μL, 0.49 mmol), ethyl acrylate (52 μL, 0.49 mmol), and 2 mL of benzene were added by syringe under an argon blanket. The reaction mixture was degassed and then backfilled with O_2. The reaction mixture was heated to 60 °C for 6 h then filtered through a pad of Celite. The filtrate was concentrated under reduced pressure, then washed with H_2O (5 mL). The organic materials were extracted with hexanes (3 × 5 mL), and then concentrated in vacuo. The residue was purified by flash chromatography on silica gel using a 95:5 hexanes/EtOAc mixture. Reported isolated yields are the average of two runs. ^{1}H NMR spectra and GCMS data for ethyl cinnamate produced by this method are provided as Supporting Information.

(b). In Situ Mixing of Pd(OAc)$_2$ and 2,5-Mes$_2$py. In the glovebox, a 25 mL Teflon-capped reaction vessel was charged with $Pd(OAc)_2$ (0.014 g, 0.06 mmol, 10 mol %) and $2,5\text{-Mes}_2\text{py}$ (0.038 g, 0.12 mmol, 20 mol %) and a magnetic stir bar. The vessel was attached to an argon-charged Schlenk line, and acetic anhydride (57 μL, 0.60 mmol), ethyl acrylate (64 μL, 0.60 mmol), and 2 mL of benzene were added by syringe under an argon blanket. The reaction, workup, and isolation were conducted as described above. Reported isolated yields are the average of two runs.

Crystallographic Structure Determinations. Single crystal X-ray structure determinations were carried out at low temperature on a Bruker P4, Platform or Kappa Diffractometer equipped with a Bruker APEX detector. All structures were solved by direct methods with SIR 2004[53] and refined by full-matrix least-squares procedures utilizing SHELXL-97.[54] Crystallographic data collection and refinement information is listed in Supporting Information, Table S1. The crystal structure of $2,5\text{-Mes}_2\text{py}$ (Supporting Information, Figure S3) suffered from end-over-end positional disorder of the nitrogen atom and *para*-CH group. This disorder was modeled with 50% occupancy of the N and (CH) in each site and refined.

■ ASSOCIATED CONTENT

Supporting Information. Experimental procedures for thermolysis reactions and equilibrium constant determinations, results of benzene-olefination reactions, disorder model for 2, $5\text{-Mes}_2\text{py}$, crystallographic data information, CSD search criteria, and crystallographic information files (PDF and CIF). This material is available free of charge via the Internet at http://pubs.acs.org.

■ AUTHOR INFORMATION

Corresponding Author
*E-mail: jsfig@ucsd.edu.

■ ACKNOWLEDGMENT

We are grateful to the U.S. National Science Foundation for support through a CAREER Award (CHE-0954710). J.S.F. is a Cottrell Scholar of Research Corporation and an Alfred P. Sloan Research Fellow (2011-2013). We thank Dr. Stacey Brydges for helpful comments concerning ligand design.

■ REFERENCES

(1) Bosch, E.; Barnes, C. L. *Inorg. Chem.* **2001**, *40*, 3234–3236.
(2) Pell, T.; Mills, D. P.; Blake, A. J.; Lewis, W.; Liddle, S. T. *Polyhedron* **2010**, *29*, 120–125.
(3) $\text{CuI}(2,6\text{-Me}_2\text{py})_2$: Healy, P. C.; Pakawatchai, C.; White, A. H. *J. Chem. Soc., Dalton Trans.* **1983**, 1917–1927.
(4) $[\text{Ag}(2,6\text{-Me}_2\text{py})_2]\text{NO}_3$: Engelhardt, L. M.; Pakawatchai, C.; White, A. H.; Healy, P. C. *J. Chem. Soc., Dalton Trans.* **1985**, 117–123.
(5) $[\text{Cu}(2,6\text{-Me}_2\text{py})_2]\text{X}$ (X = $[BF_4]^-$, $[PF_6]^-$, $[ClO_4]^-$): Habiyakare, A.; Lucken., E. A. C.; Bernardinelli., G. *J. Chem. Soc., Dalton Trans.* **1991**, 2269–2273.
(6) $[\text{Cu}(2,6\text{-Me}_2\text{py})_3]PF_6$: Habiyakare, A.; Lucken., E. A. C.; Bernardinelli., G. *J. Chem. Soc., Dalton Trans.* **1992**, 2591–2599.
(7) *trans*-$\text{PdCl}_2(2,6\text{-Me}_2\text{py})_2$: Losier, P.; MacQuarrie, D. C.; Zaworotko, M. J. *J. Chem. Crystallogr.* **1996**, *26*, 301–303.
(8) *trans*-$\text{Pd(OAc)}_2(2,6\text{-Me}_2\text{py})_2$: Halligudi, S. B.; Bhatt, K. N.; Khan, N. H.; Kurashy, R. I.; Venkatsubramanian, K. *Polyhedron* **1996**, *15*, 2093–2101.
(9) Bips, U.; Elias, H.; Hauroeder, M.; Kleinhans, G.; Pfeifer, S.; Wannowius, K. J. *Inorg. Chem.* **1983**, *22*, 3862–3865.
(10) For an articulation of the concept of steric pressure in 2,6-disubstituted aryl ligands, see: Smith, R. C.; Shah, S.; Urnezius, E.; Protasiewicz, J. D. *J. Am. Chem. Soc.* **2003**, *125*, 40–41.
(11) Twamley, B.; Haubrich, S. T.; Power, P. P. *Adv. Organomet. Chem.* **1999**, *44*, 1–65.
(12) Robinson, G. H. *Acc. Chem. Res.* **1999**, *32*, 773–782.
(13) Clyburne, J. A. C.; McMullen, N. *Coord. Chem. Rev.* **2000**, *210*, 73–99.
(14) Rivard, E.; Power, P. P. *Inorg. Chem.* **2007**, *46*, 10047–10064.
(15) Ellison, J. J.; Power, P. P. *J. Organomet. Chem.* **1996**, *526*, 263–267.
(16) Ni, C.; Power, P. P. *Struct. Bonding (Berlin)* **2010**, *136*, 59–111.
(17) Kays, D. L. *Dalton Trans.* **2011**, 769–778.
(18) (a) Du, C. F.; Hart, H.; Ng, K. D. *J. Org. Chem.* **1986**, *52*, 3162–3165. (b) Ruhlandt-Senge, K.; Ellison, J. J.; Wehmschulte, R. J.; Pauer, F.; Power, P. P. *J. Am. Chem. Soc.* **1993**, *115*, 11353–11357.
(19) Kays, D. L.; Cowley, A. R. *Chem. Commun.* **2007**, 1053–1055.
(20) Mononuclear complexes of the formulation $M(Ar)_2$ have also been prepared with the Mes* σ-aryl ligand (Mes* = 2,4,6-(t-Bu)$_3$C$_6$H$_2$; M = Mn, Fe). See: (a) Wehmschulte, R. J.; Power, P. P. *Organometallics* **1995**, *14*, 3264–3267. (b) Müller, H.; W. Siedel, W.; Görls, H. *Angew. Chem., Int. Ed.* **1995**, *34*, 325–327.
(21) Schiemenz, B.; Power, P. P. *Angew. Chem., Int. Ed.* **1996**, *35*, 2150–2152.
(22) Mononuclear $M(Ar)_2$ complexes featuring the $2,6\text{-Dipp}_2C_6H_3$ ligand are also known (M = Mn, Fe, Co). See: (a) Ni, C.; Fettinger, J. C.; Long, G. J.; Power, P. P. *Dalton Trans.* **2010**, *39*, 10664–10670. (b) Ni, C.; Power, P. P. *Chem. Commun.* **2009**, 5543–5545. (c) Ni, C.; Stich, T. A.; Long, G. J.; Power, P. P. *Chem. Commun.* **2010**, *46*, 4466–4468. (d) Ni, C.; Hao Lei, H.; Power, P. P. *Organometallics* **2010**, *29*, 1988–1991.
(23) Nguyen, T.; Sutton, A. D.; Brynda, M.; Fettinger, J. C.; Long, G. J.; Power, P. P. *Science* **2005**, *310*, 844–847.

(24) Brynda, M.; Gagliardi, L.; Widmark, P. O.; Power, P. P.; Roos, B. O. *Angew. Chem., Int. Ed.* **2006**, *45*, 3804–3807.
(25) Wolf, R.; Ni, C.; Nguyen, T.; Brynda, M.; Long, G. J.; Sutton, A. D.; Fischer, R. C.; Fettinger, J. C.; Hellman, M.; Pu, L.; Power, P. P. *Inorg. Chem.* **2007**, *46*, 11277–11290.
(26) La Macchia, G.; Gagliardi, L.; Power, P. P.; Brynda, M. *J. Am. Chem. Soc.* **2008**, *130*, 5104–5114.
(27) Ni, C.; Ellis, B. D.; Long, G. J.; Power, P. P. *Chem. Commun.* **2009**, 2332–2334.
(28) Saito, Y.; Takemoto, J.; Hutchinson, B.; Nakamoto, K. *Inorg. Chem.* **1972**, *11*, 2003–2011.
(29) Based on their respective hydrides, the sum of the covalent radii for Ag (1.26 Å) and O (0.73 Å) is 1.99 Å. See, Batsanov, S. S. *Rus. Chem. Bull.* **1995**, *45*, 2245–2250.
(30) Reynoso-Paz, C. M.; Olmstead, M. M.; Kurth, M. J.; Schore, N. E. *Acta Crystallogr.* **2002**, *E58*, m310–m312.
(31) Cambridge Structural Database (CSD v. 5.32, Nov. 2010); Allen, F. H. *Acta Crystallogr.* **2002**, *B58*, 380–388; See the Supporting Information for search criteria.
(32) An alternative proposal for this minor product is the bridging acetate dimer, $[\mu\text{-}(\kappa^2\text{-OAc})\text{Pd(OAc)}(2,5\text{-Mes}_2\text{py})]_2$. However, this dimeric species would show two distinct acetate resonances, or exhibit a 2:1 ratio of acetate to 2,5-Mes_2py ^{1}H resonances if the bridging and terminal acetate ligands were in rapid exchange. See ref 33.
(33) Zhang, Y.-H.; Shi, B.-F.; Yu, J.-Q. *J. Am. Chem. Soc.* **2009**, *131*, 5072–5074.
(34) For some examples of other Pd-mediated C-H activation reactions featuring neutral, N-donor ligands, see the following and refs 35−36: Ackerman, L. J.; Sadighi, J. P.; Kurtz, D. M.; Labinger, J. A.; Bercaw, J. E. *Organometallics* **2003**, *22*, 3884.
(35) Bercaw, J. E.; Hazari, N.; Labinger, J. A.; Oblad, P. F. *Angew. Chem., Int. Ed.* **2008**, *47*, 9941–9943.
(36) Butschke, B.; Schwarz, H. *Organometallics* **2011**, *30*, 1588–1598.
(37) The *trans*- isomer is formed exclusively. See the Supporting Information.
(38) In the absence of 2,5-Mes_2py, Pd(OAc)_2 couples benzene to ethyl acrylate in 11% isolated yield under identical conditions.
(39) Yokota, T.; Tani, M.; Sakaguchi, S.; Ishii, Y. *J. Am. Chem. Soc.* **2003**, *125*, 1476–1477.
(40) Dams, M.; De Vos, D. E.; Celen, S.; Jacobs, P. A. *Angew. Chem., Int. Ed.* **2003**, *42*, 3512–3515.
(41) Ferreira, E. M.; Stoltz, B. M. *J. Am. Chem. Soc.* **2003**, *125*, 9578–9579.
(42) Zhang, H.; Ferreira, E. M.; Stoltz, B. M. *Angew. Chem., Int. Ed.* **2004**, *43*, 6144–6148.
(43) Grimster, N. P.; Gauntlett, C.; Godfrey, C. R. A.; Gaunt, M. J. *Angew. Chem., Int. Ed.* **2005**, *44*, 3125–3129.
(44) For a thorough discussion of electronic and geometric structure relationships in pseudotetrahedral d^7 Co(II) complexes, see: Jenkins, D. M.; Peters, J. C. *J. Am. Chem. Soc.* **2005**, *127*, 7148–7165.
(45) See the Supporting Information for details. $K_{eq} = ([\mathbf{6}]^2/([2,5\text{-Mes}_2\text{py}]^2[\mathbf{5}])$, where **6** = $\text{CoI}_2(2,5\text{-Mes}_2\text{py})_2$. ^{1}H NMR integration vs Cp_2Fe internal standard.
(46) An ideal tetrahedral geometry gives rise to a τ_4 value of 1.0, see: Powell, D. R.; Houser, R. P. *Dalton Trans.* **2007**, 955–964; The τ_4 value for $\text{CoI}_2(2,5\text{-Mes}_2\text{py})_2$ is the average for two crystallographically independent molecules (τ_4 = 0.77 and 0.82).
(47) Singh, P. P.; Srivatava, S. K.; Srivatava, A. K. *J. Inorg. Nucl. Chem.* **1980**, *42*, 521–532.
(48) Yamamoto, Y. *J. Org. Chem.* **2007**, *72*, 7817–7831.
(49) Efforts to crystallographically characterize **8** have thus far been unsuccessful, but we suspect that its structure is similar to that of bridging diiodide **5**.
(50) Connelly, N. G.; Hicks., O. M.; Lewis, G. R.; Orpen, A. G.; Wood, A. J. *Dalton Trans.* **2000**, 1637–1643.
(51) The related, four-coordinate trihalo anions, $[\text{CoX}_3(\text{THF})]^-$ (X = Cl, Br, I) have been structurally characterized. See for example: (a) $[\text{CoCl}_3(\text{THF})]^-$: Heinze, K.; Huttner, G.; Zsolnai, L.; Schober, P. *Inorg. Chem.* **1997**, *36*, 5457–5469. (b) $[\text{CoBr}_3(\text{THF})]^-$: Hilt, G.; Hess, W.; Harms, K. *Synthesis* **2008**, 75–78. (c) $[\text{CoI}_3(\text{THF})]^-$: Herbst, K.; Soderhjeim, E.; Nordlander, E.; Dahlenburg, L.; Brorson, M. *Inorg. Chim. Acta* **2007**, *360*, 2697–2703.
(52) Fulmer, G. R.; Miller, A. J. M.; Sherden, N. H.; Gottlieb, H. E.; Nudelman, A.; Stoltz, B. M.; Bercaw, J. E.; Goldberg, K. I. *Organometallics* **2010**, *29*, 2176–2179.
(53) Burla, M. C.; Caliandro, R.; Camalli, M.; Carrozzini, B.; Cascarano, G. L.; De Caro, L.; Gaicovazzo, C.; Polidori, G.; Spagna, R. *J. Appl. Crystallogr.* **2005**, *38*, 381–388.
(54) Sheldrick, G. M. *Acta Crystallogr.* **2008**, *A64*, 112–122.